Ecological Modelling 291 (2014) 183–192

Contents lists available at ScienceDirect

Ecological Modelling

journal homepage: www.elsevier.com/locate/ecolmodel

Long-term prediction of grassland production for five temporal patterns of precipitation during the growing season of plants based on a system model in Xilingol, Inner Mongolia, China

Yiruhan[a,b,*], Masae Shiyomi[a,c,g], Tsuyoshi Akiyama[d], Shiping Wang[e], Yasuo Yamamura[f], Yoshimichi Hori[g], Ailikun[h]

[a] School of Environment, Jinan University, Guangzhou 510632, China
[b] Key Laboratory of Water/Soil Toxic Pollutants Control and Bioremediation, Department of Education of Guangdong Province, Guangzhou 510632, China
[c] The Open University of Japan, Ibaraki Study Center, Bunkyo, Mito, Japan
[d] Gifu University, Professor Emeritus, Gifu, Japan
[e] Institute of Tibetan Plateau Research, Chinese Academy of Sciences, Beijing, China
[f] Ibaraki University, School of Science, Bunkyo, Mito, Japan
[g] Ibaraki University, Professor Emeritus, Bunkyo, Mito, Japan
[h] Institute of Atmospheric Physics, Chinese Academy of Science, Beijing, China

ARTICLE INFO

Article history:
Received 4 May 2014
Received in revised form 17 July 2014
Accepted 21 July 2014
Available online 23 August 2014

Keywords:
Arid/semiarid steppe
Cluster analysis
Drought year
Grassland production
Grazing
Precipitation

ABSTRACT

We proposed a method to conveniently predict seasonal changes in aboveground grassland biomass in Xilingol, Inner Mongola, China, by herders and their cooperative. First, we formed five precipitation patterns with different meteorological characteristics during the plant growing season (March 16–October 15) using data accumulated for 55 years since 1953 at the Xilinghot Meteorological Observatory based on cluster analysis. Second, we applied the improved Xilingol Grassland Ecosystem Model to each of the five precipitation patterns and the 55-year grand mean of the patterns. The time-dependent aboveground biomass simulation showed different shapes among the six meteorological patterns, in particular a pattern formed by 13 drought years that produced the lowest aboveground biomass during the entire plant growing season. At the beginning of grazing season, herders and/or their cooperatives can choose one of the six patterns based on the long- and medium-term meteorological prediction officially announced by the meteorological observatory to predict temporal changes in aboveground biomass during a growing season of grassland plants. As the drought pattern years will come statistically once in four years in the Xilingol area according to our study, maintaining an appropriate stocking density is important to avoid economic loss to herders and degradation of the grassland ecosystem. Thus, a decision for grassland utilization based on our model choice will play a key role to maintain a stable income and to avoid overgrazing and to conserve grassland vegetation.

1. Introduction

The Xilingol grassland consists of natural pastures with the highest productivity and quality in northern China. The area has been used traditionally for nomadic farming of sheep, goats, horses, and cattle and has played an important role in herders' lives and as a local industry. However, rapid economic development and population growth since the 1980s have created a demand for increased agricultural production. The rising need for agricultural products has resulted in higher stocking density and increased cultivation of the Xilingol grasslands, generating a shift in agricultural policy from nomadism to stationary farming in the late 1980s. This development has triggered a biological succession of partial degradation and desertification of the grasslands (e.g., Yiruhan et al., 2001; Tong et al., 2004; He et al., 2005; Akiyama and Kawamura, 2007; Li et al., 2007; Liu and Wang, 2007). The annual temperature rise in the steppe (temperate arid/semiarid grasslands) has been much more intense than that in other humid temperate areas and has been estimated to be >2 °C during the past 50 years (Yiruhan et al., 2011; Wuyunna et al., 2012).

Precipitation is the primary factor limiting plant production in arid/semiarid regions under conditions of proper soil fertility and stocking density (Hooper and Johnson, 1999; Swemmer et al.,

* Corresponding author at: School of Environment, Jinan University, Guangzhou 510632, China. Tel.: +86 20 85226615; fax: +86 20 85226615.
E-mail address: tyiruhan@jnu.edu.cn (Yiruhan).

http://dx.doi.org/10.1016/j.ecolmodel.2014.07.018
0304-3800/

2007; Deshmukh, 2008; Heislar-White et al., 2008). That is, when precipitation is sufficient in arid/semiarid regions, plant growth is high, whereas plant growth is low during dry weather. This relation between meteorology and plant growth is rather simple, that is, the effects of temperature on grassland production are considerably smaller compared to those of precipitation (Parton, 1978). We suppose that grassland ecosystems are constructed by a system of interacting plant communities, meteorological factors, soil conditions, and anthropogenic factors (such as grazing, cutting, and fertilizing). We have studied a dynamic grassland ecosystem model in the Xilingol steppe, Inner Mongolia (Shiyomi et al., 2011). We can simulate dynamic changes in aboveground biomass (AGB), belowground biomass, and livestock body weight grazed under a condition of varying meteorological conditions using this model, i.e., a so-called van Dyne-type model (van Dyne, 1969). Simulated results based on the system model are sensitive to meteorological conditions such as temperature and precipitation during the plant growing season (Shiyomi et al., 2011).

Daily meteorological data including daily temperature and precipitation have been accumulated at the Xilingol Meteorological Observatory since 1952. Although these data tend to vary annually, their tendencies can be summarized into several patterns that change over time. In this report, we propose a method for easily predicting AGB based on several meteorological patterns and the model, which was improved to be proper to grazing. First, we developed several seasonal precipitation patterns, which comprise the primary limiting factor for producing AGB in a semiarid region.

Second, we simulated the seasonal changes in AGB by applying our system model and the precipitation patterns. Individual herders (or their cooperative) determine which precipitation pattern will occur during the new season according to the medium-/long-term meteorological prediction, and then they choose one AGB pattern from the precipitation patterns for the grassland of the new season. If this method is successful, it will be unnecessary for herders and their cooperative to measure environmental conditions such as soil temperature, precipitation, and soil water content for model calculations, because they will be able to predict biomass production only by choosing one pattern from the given meteorological patterns without these measurements. To predict whether the grasslands maintain sufficient biomass for a given stocking density, and for rationally managing the grassland, will contribute to increasing their living standard, enhance environmental conservation, and maintain and improve the local economy.

The present report had several objectives, as follows:

(1) To describe the dynamic model and factors involved in constructing grassland producing systems;
(2) To develop several seasonal change patterns of monthly precipitation during the plant growing season using cluster analysis and data accumulated by the Xilingol Meteorological Observatory;
(3) To calculate grassland AGB for each changing pattern of precipitation; and
(4) To choose a meteorological pattern based on medium-/long-term meteorological prediction, and to determine temporal changes in the AGB corresponding to the chosen meteorological prediction.

2. Materials and methods

2.1. The target region

The target region of this study was sheep grazing grassland located at the Inner Mongolia Grassland Ecosystem Research Station, Institute of Botany, Chinese Academy of Science (43°32′ N, 116°40′ E, 1100 m a.s.l.; hereafter referred to as the Station), about 30 km northwest of Xilinhot City (the capital of Xilingol) (Fig. 1; Chen and Wang, 2000). The area contains calcic chestnut soil with a pH of 7.2–8.7 (Chen and Wang, 2000). The organic matter content and total nitrogen in the soil were 103.8 g kg^{-1} and 6.04 g kg^{-1}, respectively (Chen and Wang, 2000). The average annual air temperature recorded at the Station from 1990 to 1998 was 1.0 °C. January was the coldest month (average, −21.1 °C) and July was the warmest (average, 18.7 °C). The average yearly precipitation from 1982 to 1998 was 350 mm (range, 182–507 mm). Most precipitation occurs between June and September, and the annual potential evaporation is 403 mm. The annual mean duration of sunshine was 2617 h (range, 2267–2883 h) (Chen and Wang, 2000; Huang et al., 2004). The dominant plant species are *Leymus chinensis* and *Artemisia frigida* (Chen and Wang, 2000; Chen et al., 2008).

Fig. 1. Modeling target area (Xilingol, Inner Mongolia, China; 43°32′ N, 116°40′ E, 1100 m a.s.l.). Meteorological data were collected at the Xilingol Meteorological Observatory in the Xilinhot City (about 30 km southeast of the modeling target area)

The entire experimental pasture was divided into five 3-ha blocks. Each block was further divided into three 1-ha sub-blocks, and sheep were grazed in rotation three times between May 20 and October 10 (grazing season) each year. The minimum and maximum stocking densities were 1.33 and 6.7 head·(3 ha)$^{-1}$ during the grazing season (Wang et al., 1998; Wang, 2000). In the following simulations, we refer to 2.67 head·(3 ha)$^{-1}$, or 0.9 head ha^{-1}, of sheep as “standard grazing”.

2.2. Model outline

We basically used the Xilingol Grassland Model (Shiyomi et al., 2011), which was slightly improved to be sensitive to the interaction between meteorological phenomena and AGB, and to the digestibility of pasture plants. The model outline is as shown in Fig. 2. Solar energy in pasture plants is fixed by photosynthesis, a portion of the aboveground parts (such as leave and stems) is eaten by sheep, and most of the remainder accumulates as the belowground part. The aboveground portions eaten by sheep are used for sheep growth, metabolic energy, or kinetic energy, and the remainder are excreted. The energy in the aboveground part that is not eaten and is not utilized to maintain the plant is consumed by locusts and rodents or becomes standing dead material. The standing dead plant material and feces accumulate as soil organic matter, and the soil organic matter is decomposed by soil microorganisms over time.

In the model, energy inflow to and outflow from the grassland ecosystem are expressed as “source” and “sink” by flag-like shapes in Fig. 2, respectively. The ecosystem model includes five state

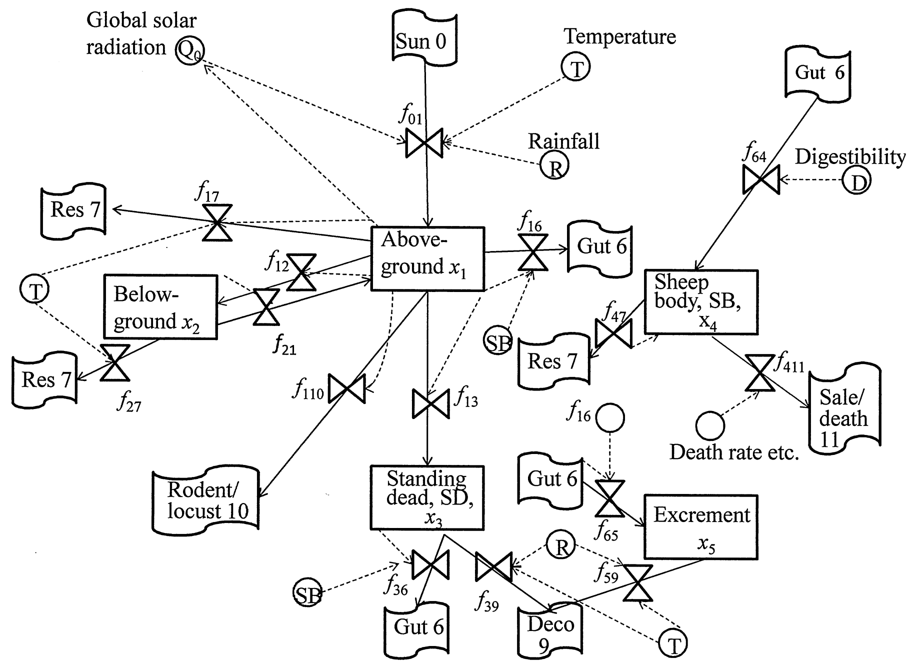

Fig. 2. Outline of the Xilingol grassland ecosystem model (modified after Shiyomi et al., 2011). The five rectangles represent state variables (x_1–x_5 matter stocks), and flags indicate sources and sinks of dry matter flow (source and sink face different directions in shape); solid arrows denote the direction of matter flow, and dashed arrows indicate the effects of parameters affecting matter flow; circles denote environmental and artificial factors directly or indirectly affecting matter flow. f_{ij} is a parameter expressing matter flow from a state variable (or source) i to another state variable (or sink) j. The following abbreviations are used: D, digestibility; Deco, decomposition; Gut, gut of sheep; Q_0, global solar radiation; P, precipitation; T, temperature; Res, respiration; SB, sheep body weight; SD, standing dead material.

variables, which are functions of time t: the amount of AGB, $x_1(t)$ (kg dry weight ha^{-1}; hereafter expressed as x_1; expressed dry weight as dw); the amount of belowground biomass, x_2 (kg dw ha^{-1}); the amount of standing dead material, x_3 (kg dw ha^{-1}); livestock body weight, x_4 (kg live weight ha^{-1}; hereafter, expressed live weight as lw); and excreta x_5 (kg dw ha^{-1}). Energy is expressed as dry (for plant and excreta) or live (for livestock) weight (kg) of carbohydrate instead of joules. The transport of energy (carbohydrate) between state variables, from a source to a state variable, and from a state variable to a sink, is expressed by f_{ij}, where i and j indicate the exit and entrance of the energy flow, respectively, and f_{ij} is also a function of t. All f_{ij}s should be estimated based on experiments before modeling. However, as estimating so many f_{ij}s in experiments was difficult, some of them were cited from references and our personal experience (see Shiyomi et al., 2011).

The concept shown in Fig. 2 is described by the following five differential equations:

$$\begin{aligned}
dx_1 &= (f_{01} + f_{21} - f_{12} - f_{13} - f_{16} - f_{17} - f_{110})dt,\\
dx_2 &= (f_{12} - f_{21} - f_{27})dt,\\
dx_3 &= (f_{13} - f_{36} - f_{39})dt,\\
dx_4 &= (f_{64} - f_{411} - f_{47})dt,\\
dx_5 &= (f_{65} - f_{59})dt,
\end{aligned} \tag{1}$$

The main f_{ij} values (see Fig. 2 for f_{ij}) were summarized as follows:

(1) Daily energy fixation rate through photosynthesis, is expressed as f_{01} (unit: dw kg ha^{-1} day^{-1}), which is determined from the daily amount of solar radiation, daily precipitation, and daily mean air temperature.
(2) Daily respiration rate of the aboveground plant parts, f_{17} (dw kg ha^{-1} day^{-1}), is a function of the daily mean air temperature.
(3) Daily intake by sheep (f_{16}; dw kg ha^{-1} day^{-1}) is $f_{16} = 0.043w$ for the live body weight of a sheep (w kg) when the available amount of herbage (x_1) is more than that of the herbage amount required; daily intake is $f_{16} = 0.2x_1$, when the available amount of herbage (x_1) is less than that of the herbage amount required.
(4) Daily consumption by locusts and rodents (f_{110}; dw kg ha^{-1} day^{-1}) is 0 at present, but we can use any value.
(5) Daily death rate of AGB (f_{13}; dw kg ha^{-1} day^{-1}) is given based on Chen and Wang (2000), as a small value from spring to summer and a large value in autumn.
(6) The daily body weight increase rate per sheep is given as 100 g, when the available amount of herbage is larger than that required; body weight decreases when the amount of herbage available is insufficient.
(7) The digestibility of herbage plants is 0.65 through the entire grazing season.

Detailed information regarding the other f_{ij}s is almost the same as values given in Shiyomi et al. (2011). In this report, plant growth was affected by the meteorological conditions after March 16. Although excrement (x_5) and standing dead material of plants (x_3) are included in the model and the simulations, we omitted the detailed explanation here because these statements are not important for the following discussion.

In the simulations, the initial AGB on April 1 was given as 200 dw kg ha^{-1} in the standard cases based on Wang et al. (1998). In the simulations to evaluate the effect of initial AGB value on April 1, four different initial values were tried.

Grazing started on May 20 each year at this Station. The initial stocking density on May 20 was set to 0.9 head ha^{-1}, assuming each sheep for “standard grazing” is 40 kg. Although rotational grazing was adopted in the field experiments for this modeling study (Wang et al., 1998), we tried continuous grazing in the simulations because rotational grazing is difficult to set in our software to analyze differential equations. For example, we adopted continuous grazing of 0.9 head ha^{-1} for rotational grazing of 2.67 head·(3 ha)$^{-1}$. Here we comment on difference between continuous and rotational grazing. Comparisons of continuous and rotational grazing have been conducted based on many field experiments since 1950s. Experimental results show that continuous grazing is similar to rotational grazing in plant production, but most rotational grazing is superior to continuous grazing in animal production (Davis and Pratt, 1956; Walton et al., 1981; Lantinga, 1985). Today, in intensively managed sown grassland rotational grazing is common (Hodgson and Brookes, 1999; Briske et al., 2008), but in extensively managed natural grasslands, as in Inner Mongolia, continuous grazing is still common.

2.3. Cluster analysis of years based on precipitation

Precipitation is the factor that most affects plant growth in arid/semiarid regions. The Xilingol Meteorological Observatory has accumulated official data since 1952, under the direction of the Meteorological Department of the State Council based on the Meteorological Law of the People's Republic of China. We used precipitation data recorded during 55 years (1953–2007) at the Xilinghot Meteorological Observatory (43°5′ N, 116°0′ E, 989 m a.s.l.) in Xilighot City near the Station for the cluster analysis. The period from the middle of March, when plant growth begins, to the middle of October, when plant growth ends, was divided into seven periods of 30 or 31 days, and the accumulated precipitation during each period was considered as variate. The seven periods were as follows: (1) March 16–April 15 (hereafter expressed as MA), (2) April 16–May 15 (AM), (3) May 16–June 15 (MJ), (4) June 16–July 15 (JJ), (5) July 16–August 15 (JA), (6) August 16–September 15 (AS), and (7) September 16–October 15 (SO).

After transforming daily precipitation (r) from March 16 to October 15 into $\log_{10}(r+1)$, the transformed daily precipitation data were averaged for each of the seven periods from MA to SO for each year to use in the cluster analysis. Euclidian distance was used as the distance, and k-means (Kendall, 1980) was applied as the clustering method. We classified the 55 years into five clusters of precipitation patterns (referred to as the five patterns).

2.4. Daily precipitation, precipitation days, daily air temperature, and global solar radiation used in the simulations

The AGB changes with time were calculated for each pattern, based on daily global solar radiation, daily air temperature and daily precipitation for the corresponding pattern. We first determined the mean daily precipitation (e.g., a) through the years contained in each of the five patterns. Then, we determined the intervals between the two nearest precipitation days based on random numbers considering the actual number of monthly precipitation days recorded at the observatory. The precipitation on one precipitation day in the simulation was assumed to be the total of the mean daily precipitation (a) accumulated during the two nearest precipitation days.

We assumed that the effect of one precipitation event on plant growth lasted 10 days and that the effect decreased 1/10 every day. That is, the effect of precipitation on day $t=j$ (expressed by $R_{t=j}$; referred to as the rainfall index value) for the jth day after March 16 ($t=0$) was described by the following equation:

$$R_{t=j} = \sum_{i=0}^{9} \frac{(10-i) r_{t=j-i}}{10}$$

(unit for R and r: mm day^{-1}), where $r_{t=j-i}$ is the daily precipitation on the $(j-i)$th day from March 16 ($i=0, 1, \ldots, 9$).

Mean daily temperatures for the years included in each precipitation pattern were used in the simulations for each pattern. Although global solar radiation is an important factor for primary production, we could not obtain data from the observatory. However, we were able to obtain global solar radiation data for 2 years at the Station; thus, we fitted a sine-curve to the seasonal changes in global solar radiation and used the same curve for all simulations.

2.5. Initial values for the five variables and stocking density at the beginning of the simulation

Initial values on April 1 for the four state variables for the standard grazing were as follows: AGB, 200 kg dw ha^{-1}, belowground biomass, 8845 kg dw ha^{-1}; standing dead material, 250 kg dw ha^{-1}; and excrement, 2 kg dw ha^{-1}. Livestock weight for the standard grazing was set to as follows: on March 16, 0 kg ha^{-1}, on May 20 (grazing starts) 0.9 sheep with 40 kg lw ha^{-1}, and on October 5 (grazing ends) 0 kg ha^{-1} (Wang et al., 1998; Wang, 2000).

In the simulations to evaluate the effect of the initial values on AGB, the initial AGB values on April 1 were set to 400, 200, 100, and 50 kg dw ha^{-1} under the condition that the initial values for the other variables were fixed at the same values as those for standard grazing.

We gave various initial values of 1–10 head ha^{-1} and 40 kg $head^{-1}$ as the stocking density on May 20 for simulations to evaluate the effects of stocking density on AGB, under the condition that the initial values for the other variables were fixed at the same values as those for standard grazing.

2.6. Differential equation solutions

A set of differential equations (Eq. (1)) was numerically solved using the second-order Runge–Kutta method equipped on STELLA®5.1.1(High Performing Systems, Inc., Watkinsville, GA, USA).

Besides the preceding five meteorological patterns, we showed changes in AGB for daily temperature, precipitation, and daily global solar radiation averaged over the entire 55 years (referred as to the general pattern, or pattern G).

The calculation began on April 1 and ended on October 15 for all cases.

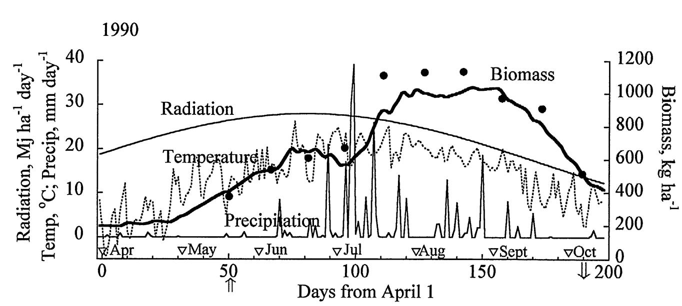

Fig. 3. Daily changes in solar radiation (the sin-curve fitted to data obtained at the Station), precipitation (Precip) and air temperature (Temp) (recorded at the Xilinghot Meteorological Observatory in 1990), simulated aboveground biomass (AGB; bold line), and AGB data (●) obtained experimentally at the Xilingol Station in 1990 (Wang et al., 1998). Grazing started on May 20 (up arrow) and finished on October 5 (down arrow) in the simulation. Downward triangles on the abscissa indicate the first day of a month. The stocking density was 0.9 head ha^{-1} and the body weight of sheep on the initial day of grazing was set to 40 kg lw $head^{-1}$. Continuous grazing was conducted. The initial AGB on April 1 was set to 200 kg dw ha^{-1}.

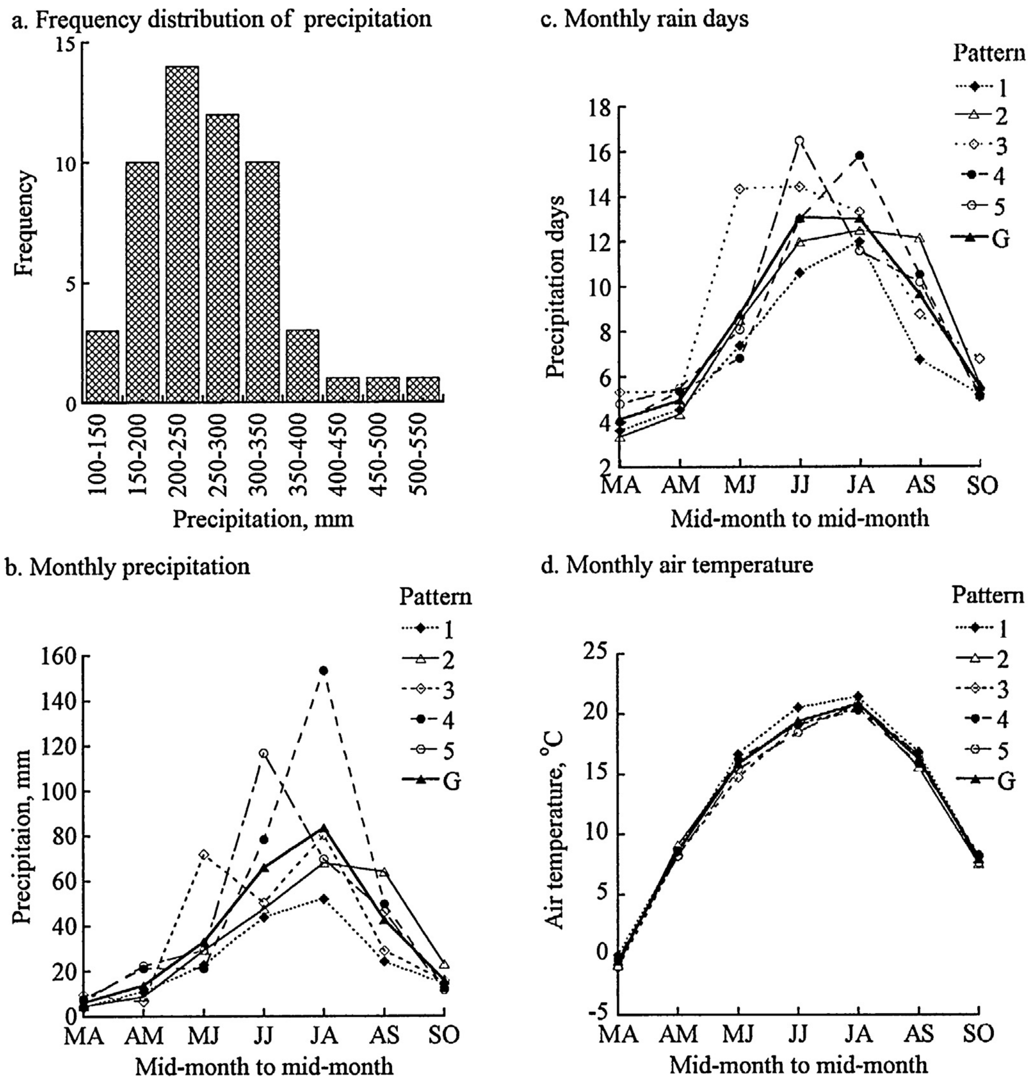

Fig. 4. Meteorological conditions, 1953–2007. (a) Frequency distribution of precipitation for the 55 plant growing seasons (March 16–October 15); (b) patterns 1–5 and the grand mean (pattern G) in monthly precipitation; (c) monthly days of precipitation for patterns 1–5 and G; (d) monthly temperature for patterns 1–5 and G. MA, March 16–April 15; AM, April 16–May 15; MJ, May 16–June 15; JJ, June 16–July 15; JA, July 16–August 15; AS, August 16–September 15; SO, September 16–October 15.

3. Results

3.1. Changes in simulated and observed AGBs with time

The original model reported previously reproduced the actual changes in AGB at the Station under several different years and for several different grazing conditions (Shiyomi et al., 2011). Here, we show only one example of well-reproduced experimental results for AGB in 1990 in which 0.9 head of sheep at 40 kg head^{-1} began grazing on May 10 under the 1990 meteorological conditions (Fig. 3).

3.2. Cluster analysis of years based on monthly precipitation from March 16 to October 15

Fig. 4a shows the frequency distribution of total precipitation from March 16 to October 15 at the observatory during the 55 years. The minimum was 108.6 mm in 2005, and the maximum was 541.4 mm in 1954. Three years had precipitation <150 mm, and three years had >400 mm.

Fig. 4b shows cluster analysis results (i.e., the five precipitation patterns) based on monthly precipitation (from a mid-month to the next mid-month), and Table 1 shows the characteristics of each pattern and the number of years in each pattern. Nine to thirteen years were contained in each of the five patterns.

Pattern 1 had little precipitation after April. Pattern 2 had slightly less precipitation to that of pattern G during the first half of the growth period but slightly more precipitation during the second half of the growth period. Pattern 3 had two peaks of precipitation in MJ and JA. Pattern 4 showed the most precipitation in JA, and pattern 5 showed the most precipitation in JJ. The number of precipitation days was similar to precipitation (Fig. 4c). No large differences in temperature were detected between patterns except for pattern 1 with high temperatures from MJ to AS, and pattern 5 with slightly lower temperatures from MA to JJ (Fig. 4d).

Table 2 shows the total precipitation, number of precipitating days, and daily mean precipitation when it was rainy, during the growing season (March 16–October 15) for each pattern. Patterns 4 and 5 showed high daily and total precipitation values, whereas pattern 1 showed low values for both total and daily precipitation. Patterns 2 and 3 had intermediate values between pattern 1 and patterns 4 and 5. The bottom one row in Table 2 indicates the year (2005; contained in pattern 1) with the least amount of precipitation in the growing seasons during the 55 years.

Table 1
The meteorological characteristics in the five precipitation patterns and years constructing each pattern.

Pattern	Precipitation	Precipitation days	Temperature	Years (last two figures)
1	Except for MA, SO: very low	Except for SO: few	MJ-AS: very high	13 years: 1953, 65, 68, 72, 80, 82, 85, 94, 2000, 01, 02, 05, 07
2	JJ, JA: low; AS, SO: high	AS: many	AS: a little low	12 years: 1958, 61, 64, 66, 69, 71, 73, 83, 84, 86, 89, 95
3	MJ: high; AS: low	MJ, JJ: many; AS: few	MJ: a little low	9 years: 1957, 60, 67, 76, 77, 78, 91, 97, 2006
4	JJ: high; JA: very high	JA: many	JA: a little low	11 years: 1954, 63, 74, 79, 81, 87, 88, 93, 96, 98, 2004
5	JJ: very high	JJ: many	JJ: a little low	10 years: 1955, 56, 59, 62, 70, 75, 90, 92, 99, 2003

MA: March 16–April 15; AM: April 16–May 15; MJ: May 16–June 15; JJ: June16–July 15; JA: July 16–August 15; AS: August 16–September 15; SO: September 16–October 15.

Table 2
Precipitation and precipitation days in one growing season (MA–SO), and the mean precipitation in one precipitation day.

Pattern	Precipitation (mm)	Precipitation days	Precipitation in one precipitation day (mm)	Remarks year (pattern no.)
1	172.3	50.2	3.4	
2	245.6	58.5	4.2	
3	263.7	68.3	3.9	
4	344.6	60.7	5.7	
5	303.0	61.8	4.9	
G	261.5	59.2	4.4	
Minimum[a]	108.6	41	2.6	2005 (Pattern 1)

[a] The year with the least precipitation from March 16 to October 15.

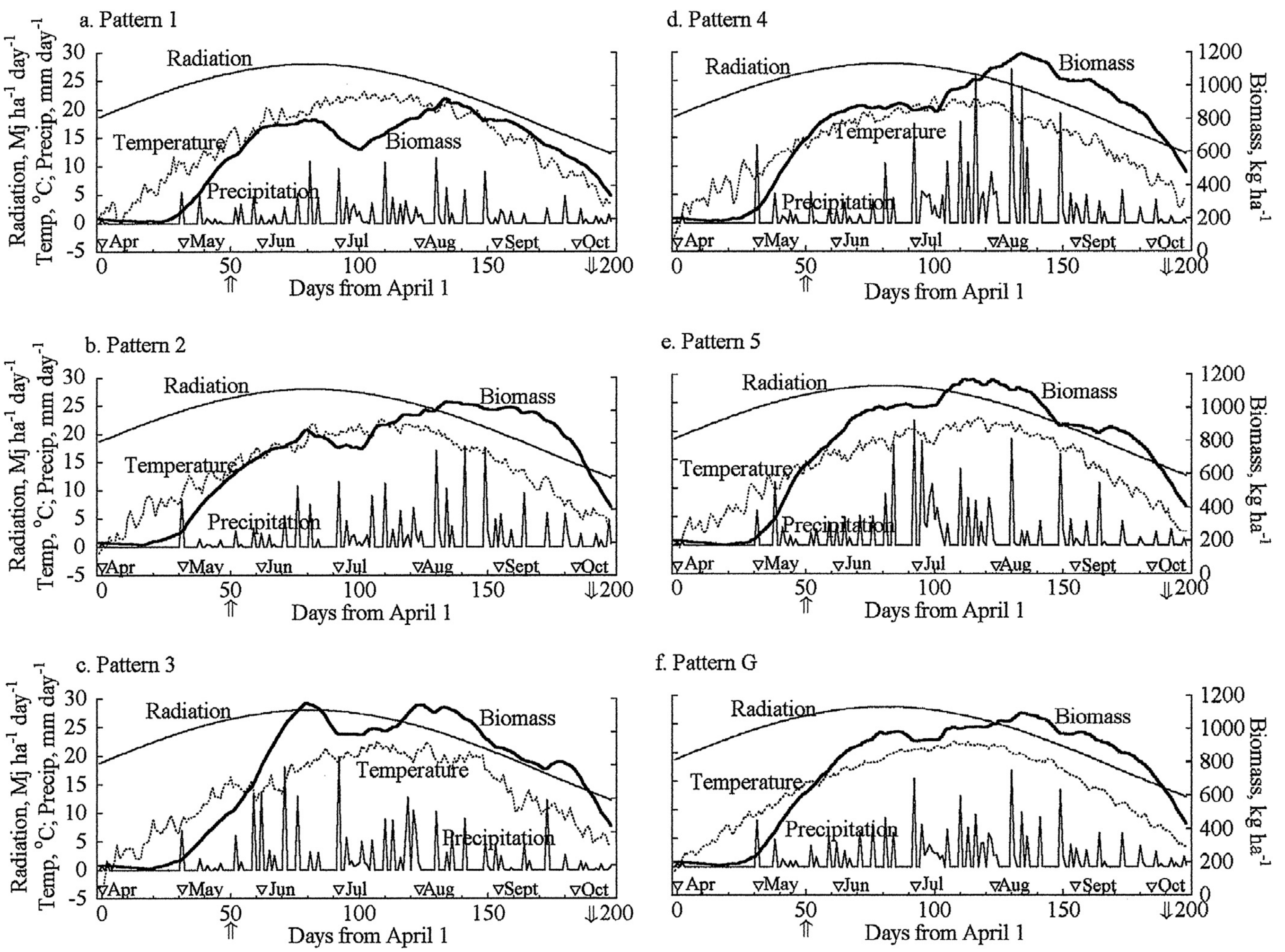

Fig. 5. Daily changes in global solar radiation (the sin-curve fitted to data obtained at the Station), precipitation and temperature (recorded at the Xilinghot Meteorological Observatory), and simulated aboveground biomass (AGB). (a) Pattern 1; (b) pattern 2; (c) pattern 3; (d) pattern 4; (e) pattern 5; (f) pattern G. See text for characteristics of temporal changes in AGB. The followings are assumed: grazing started on May 20 (up arrow) and finished on October 5 (down arrow). The stocking density was 0.9 head ha^{-1} and the body weight of sheep on the initial day of grazing was set to 40 kg lw head^{-1}. Continuous grazing was conducted. The initial AGB on April 1 was set to 200 kg dw ha^{-1}. Downward triangles on the abscissa indicate the first day of a month.

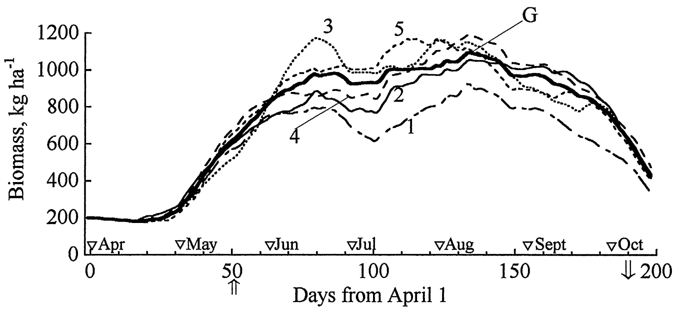

Fig. 6. Comparisons of biomass for patterns 1–5 and G (grand mean during 55 years). Numbers 1–5 and G indicate the patterns. Up and down arrows indicate the days which grazing started and ended, respectively. Downward triangles on the abscissa indicate the first day of a month.

3.3. Prediction of AGB for each meteorological pattern

Fig. 5 shows the simulated seasonal changes in AGB, for each meteorological pattern for a per-hectare stocking density of 0.9 head of sheep with a body weight of 40 kg at the beginning of grazing (referred to as “standard stocking density”) (Wang et al., 1998). The seasonal changes in AGB were different among the patterns. Biomass (AGB) increased sharply in all patterns after April and then decreased rapidly after September.

The AGB in pattern 1, which has very little amount of precipitation, was small after June, and the peak in August was around 0.9 t ha^{-1}. Pattern 2, whose characteristics were relatively high precipitation and low temperature in August, maintained high biomass in August and September, and biomass exceeded 1.0 t ha^{-1} in middle to late August. Pattern 3, which had much precipitation after June, had two peaks of biomass >1.17 t ha^{-1} that occurred in June and August. Pattern 4 showed a low biomass (0.9 t ha^{-1} level) in June because of high temperature, but the biomass reached 1.2 t ha^{-1} in August because of high precipitation in July and August. In pattern 5, precipitation after late June accelerated growth, and biomass in August was >1.15 t ha^{-1}. The characteristics of pattern G showed the average precipitation tendencies of patterns 1–5. Accordingly, pattern G had no extremely low or high precipitation during the plant growing period. These meteorological conditions in pattern G were suitable to plant growth resulting in moderate biomass in August (1.05 t ha^{-1}).

Fig. 6 shows comparisons of temporal AGB changes in patterns 1–5 and G. AGB in pattern 1 was extremely low compared to that in pattern G, and the AGBs for the other patterns were not much different from that of pattern G. These results indicate that all patterns produced a 100 g daily increase in sheep body-weight under the condition of 0.9 head ha^{-1} stocking density (body weight changes are not shown in figures).

We then used several different stocking densities from 1 to 10 head ha^{-1} (the initial body weight of each sheep on May 10 was 40 kg) to evaluate the effects of stocking density on grassland production. AGB decreased at higher stocking density, but the extent of decrease differed among the precipitation patterns. Fig. 7a and b shows the biomass changes in patterns G and 1. In pattern G (Fig. 7a), the daily body mass increase of sheep (100 g per individual) was maintained until the end of the grazing period for the 1–8 head ha^{-1} stocking density, and the AGB at the beginning of the following year was guaranteed for the 1–7 head ha^{-1}. In patterns 2–5 and G, one could achieve higher stocking densities than in pattern 1 (not shown in the figures). However, the AGB in pattern 1 was destroyed by October with the stocking density greater than 8 head ha^{-1} (shown by Italic letters in Fig. 7b) and in the stocking density greater than 6 head ha^{-1}, the AGB amounts at the beginning of the next year were not guaranteed (underlined numbers in

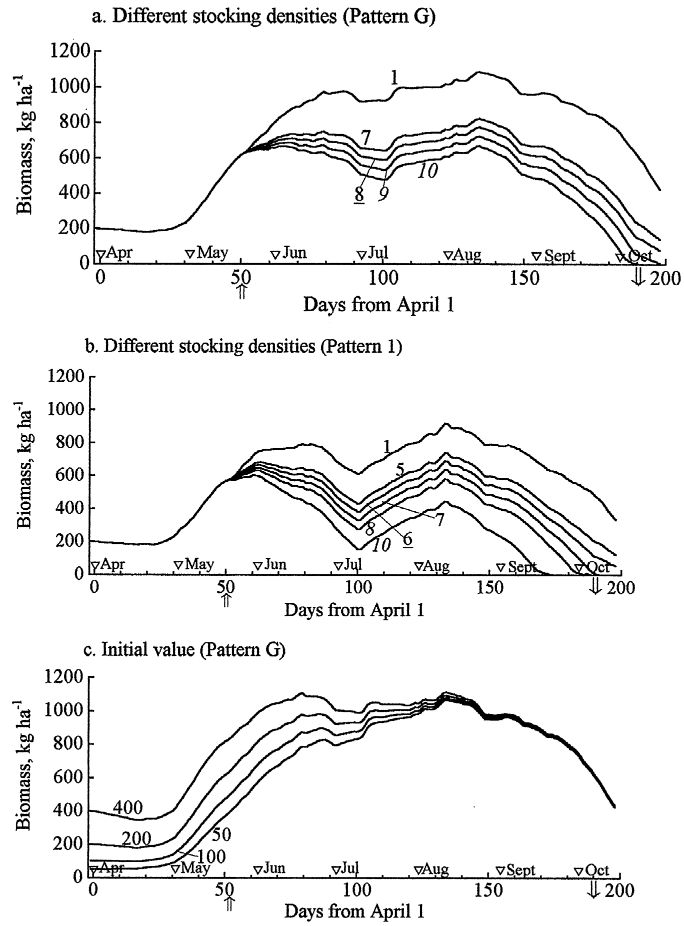

Fig. 7. Aboveground biomass (AGB) values simulated for different stocking densities and different AGBs on April 1. (a) Pattern G. (b) Pattern 1. (c) AGBs simulated for different initial values of AGB. (a) and (b) Numerals indicate stocking densities (head ha^{-1}), where body weight of individual sheep was assumed to be 40 kg at the start of grazing. Roman letters indicate that both the 100 g daily body weight increase of sheep until the end of grazing season, and the AGB amount at start of the next year, are guaranteed. Underlined numbers indicate that 100 g daily body weight increase of sheep until the end of grazing season is guaranteed, but the AGB amounts at the start of the next spring are not always guaranteed. Italic letters indicate that neither the 100 g daily body weight increase of sheep until the end of grazing season nor the AGB amount at start of the next grazing season are guaranteed. Up and down arrows indicate the days on which grazing started (May 20) and ended (September 10), respectively. Downward triangles on the abscissa indicate the first day of a month. (c) The AGBs on April 1 were assumed to be 400, 200, 100 and 50 kg dw ha^{-1} from the top of the curves. Grazing was continuous during May 20–October 5. Symbols indicate the same meanings as those in (a) and (b).

Fig. 7b). The most extreme case was observed during the driest year (2005), when only 108.6 mm of precipitation fell during the entire growing season (Table 2, Fig. 8).

Next, we considered the effect of AGB at the beginning of the plant growing season. We set four different biomasses on April 1 as 400, 200, 100, and 50 kg ha^{-1}. Fig. 7c indicates that different initial values influenced during 100 days after April 1, but thereafter, the effect became very small. Such observation was similar for any stocking density (not shown in the figures). This result can be used to regulate and determine the beginning day of grazing.

4. Discussion

4.1. What types of models are useful for grassland predictions?

The aim of modeling a grassland ecosystem in this study was so herders could conveniently predict seasonal changes in AGB based

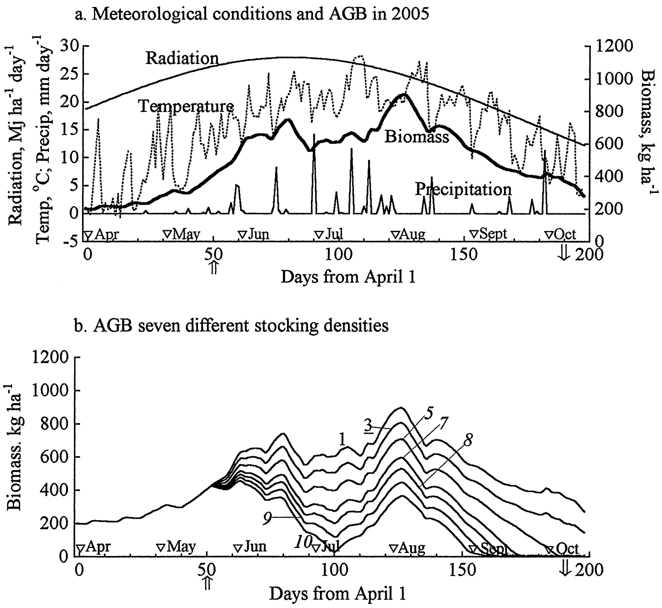

Fig. 8. Daily changes in meteorological conditions and calculated aboveground biomass (AGB) in 2005, in which precipitation was included in pattern 1 and was the least amount in the 55 years (108.6 mm from March 16 to October 15; Table 1). (a) The stocking density was assumed to be 0.9 head ha^{-1} of 40 kg lw $head^{-1}$ at the beginning of the calculation. Grazing started on May 20 and was continuous until October 10 on the computer. The initial AGB on April 1 was 200 kg dw ha^{-1}. Roman letters indicate that both the 100 g daily body weight increase of sheep until the end of grazing season, and the AGB amount at start of the next year, are guaranteed. Underlined numbers indicate that 100 g daily body weight increase of sheep until the end of grazing season is guaranteed, but the AGB amounts at the start of the next spring are not always guaranteed. Italic letters indicate that neither the 100 g daily body weight increase of sheep until the end of grazing season nor the AGB amount at start of the next grazing season are guaranteed. Up and down arrows indicate the days on which grazing started (May 20) and ended (September 10), respectively. Downward triangles on the abscissa indicate the first day of a month.

on medium- or long-term meteorological predictions. Because seasonal meteorological changes are caused by global movement of air masses, only meteorological specialists can predict them. In this report, we propose to predict grassland production (or AGB) by choosing the most suitable pattern among meteorological patterns 1–5 and G based on medium- or long-term meteorological predictions made by specialists.

Predicting grassland production is currently accomplished using data-based, statistical methods (such as multiple regression analysis), which depend strongly on remote sensing and GIS techniques (e.g., Brogaard et al., 2005; Kawamura et al., 2005; Piao et al., 2007; Butterfield and Malmström, 2009; Xie et al., 2009; Feng and Zhao, 2011). These methods are different from our prediction model. The data-based model is suitable for local or central government and policy makers who direct the production and supply of livestock feed to a large area (such as an entire province and autonomous region). In contrast, our Xilingol grassland model is a time-dependent, process-based system model that simulated a given grassland ecosystem based on the actual ecological conditions and past management in a relatively small area as the Xilingol region; therefore, the model is applicable even for a grassland ecosystem of individual herders/cooperatives in a relatively small area.

Although we only considered AGB (x_1) in this report, we can show time-dependent changes in other variables, including belowground biomass (x_2), standing dead material (x_3), livestock weight (x_4), and the amount of excreta (x_5), if necessary (Fig. 2). These variables also help supplement decisions on grassland production and maintenance. Furthermore, this type of model may be applicable to environments other than Xilingol if we change the present parameter values to those inherent in the new environment.

The time-dependent, process-based model originated from van Dyne (1969), who built a system model to analyze Colorado's Great Plains and to educate students. Such system models are also utilized widely to study production structure processes and predict production not only in grasslands but also for many crops (Torssell and Kornher, 1983; ten Berge et al., 1997; Thornley, 1998; Shiyomi et al., 2000; Huang, 2001; Scurlock et al., 2002; Zheng et al., 2006; van der Werf et al., 2007). We think that constructing a process-based model for a system contributes to the understanding, analysis, and prediction processes operating in grasslands and farmlands.

4.2. Predictability of AGB

The present model well described the seasonal changes in the actual AGB (herbage mass) (Fig. 3; Shiyomi et al., 2011). This model was sensitive to seasonal meteorological changes, particularly precipitation. Consequently, if we can appropriately predict meteorological conditions, we can predict AGB based on the model.

An excess or deficiency of herbage is determined by precipitation during the plant growing season in grasslands of arid/semiarid regions such as Xilingol. In a drought year, as shown by pattern 1 in Figs. 7 and 8, AGB will be insufficient for sheep under high stocking densities. Under conditions of relatively low stocking density such as standard grazing (0.9 head ha^{-1}) or the experiments in the Station (1.33–6.7 head·(3 ha)$^{-1}$), sufficient herbage was guaranteed under any of the meteorological patterns. However, heavier grazing, which has been progressing in the entire Inner Mongolia region, will cause a shortage of livestock feed in the grasslands and will degrade grasslands due to overgrazing. Under these circumstances, the importance of predicting AGB increases to prepare supplemental feed and/or to control stocking density.

4.3. Uncertainty of long-term meteorological predictions

A weakness exists in predicting AGB production based on medium-/long-term meteorological predictions. The use of mathematical prediction methods for precise production management is influenced by frequent, uncertain weather changes within a season, especially in temperate pluvial regions (Shiyomi, 1988; Duru and Colombani, 1992; Martin et al., 2011). Meteorological conditions incorporated into models for areas with frequent weather changes result in unstable field production predictions, even over the relatively short term (several days to a few weeks). In the semi-arid region in this modeling study, much more stable weather is expected compared to that in pluvial temperate regions. If this is true, the biomass production prediction in this region has a higher certainty compared to that in pluvial temperate regions.

4.4. Characteristics of the five meteorological patterns

The reason we classified the 55 years into five patterns for the cluster analysis of precipitation was that each pattern could contain around 10 years, which was desirable to obtain stable patterns based on our experience (the minimum was 9 years in pattern 3, Table 1).

Pattern 1, with low precipitation over the entire plant growing season, occurred in 13 of the past 55 years, i.e., 24% of the 55 years or once in 4 years. Fig. 7b indicates that AGB for pattern 1 is readily destroyed or cannot prepare a sufficient amount of biomass for the next spring if stocking density was too high. A grassland utilization plan would have to include moderate stocking densities. Damage to livestock and family/local economy would occur if the stocking density were over the limit. Thus, considering that even meteorological predictions made by authorities are inherently uncertain, too much heavy grazing should always be avoided.

All patterns except pattern 1 had high precipitation during the plant growing season, although each showed unique precipitation changes with time, e.g., peak precipitation was observed at different times during the season (Fig. 4b and c). Roughly speaking, two different AGB patterns existed based on meteorological patterns, i.e., the biomass changes in pattern 1, and those in patterns 2–5 and G. If careful management of grasslands is guaranteed when considering the differences in seasonal precipitation among patterns 2–5 and G, we can expect higher production even under a significantly higher stocking density.

4.5. Prediction of AGB

We developed five meteorological patterns and provided seasonal changes in AGB for each pattern. Herders/cooperatives would choose one of the six meteorological patterns in advance based on the medium-/long-term weather forecast. Then, they would plan allocation of land use among grazing, cutting, and protection, and determine stocking density in the grazing area based on the pattern chosen. Fig. 7 will be useful for determining their grazing plan. Herders/cooperatives can avoid considering complicated logic between meteorology and grassland organisms as well as troublesome calculations on a computer with use of the model.

The combined use of meteorological patterning and production modeling could be utilized in grasslands not only in Xilingol area but also in other areas to predict and manage grasslands if meteorological data accumulated for a long period can be obtained. Several parameter values in the model can be changed for the new area without a large modification in the model structure.

Acknowledgments

This study was funded by the Institute for Global Change Adaptation Science, Ibaraki University, Japan (ICAS) for a research on land-use and agricultural systems under the climate change, and by the Ministry of Education, Culture, Sports, Science, and Technology of Japan for a research project of "The indices for evaluating sustainable production of cropland, forest land and grassland (Project # 11490015, the Ministry of Education, Culture, Sports, Science, and Technology of Japan)"; this study was also supported by Jinan University, China, and by Ministry of Science and Technology of China (2010DFA22770). We thank these organizations and individuals involved therein.

Appendix A. Supplementary data

Supplementary data associated with this article can be found, in the online version, at http://dx.doi.org/10.1016/j.ecolmodel.2014.07.018.

References

Akiyama, T., Kawamura, K., 2007. Grassland degradation in China: methods of monitoring, management and restoration. Grassl. Sci. 53, 1–17, http://dx.doi.org/10.1111/j.1744-697X. 2007.00073.x.

Briske, D.D., Derner, J.D., Brown, J.R., Fuhlendorf, S.D., Teague, K.M., Havstad, R.L., Gillen, A.J., Ash, W., Willms, D., 2008. Rotational grazing on rangelands: reconciliation of perception and experimental evidence. Rangeland Ecol. Manage. 61, 3–17, http://dx.doi.org/10.2111/06-159R.1.

Brogaard, S., Runnström, M., Seaquist, J.W., 2005. Primary production of Inner Mongolia, China, between 1982 and 1999 estimated by a satellite data-driven light use efficiency model. Global Planet Change 45, 313–332, http://dx.doi.org/10.1016/j.gloplacha.2004.09.012.

Butterfield, H.S., Malmström, C.M., 2009. The effects of phenology on indirect measures of aboveground biomass in annual grasses. Int. J. Remote Sens. 30, 3133–3146, http://dx.doi.org/10.1080/01431160802558774.

Chen, Z.Z., Wang, S.P., 2000. Typical Grassland Ecosystems in China. Scientific Press, Beijing, pp. 4–45, 125–172, 349–358 (in Chinese).

Chen, J., Hori, Y., Yamamura, Y., Shiyomi, M., Huang, D., 2008. Spatial heterogeneity and diversity analysis of macro-vegetation in Xilingol region, Inner Mongolia, China, using beta distribution. J. Arid Environ. 72, 1110–1119, http://dx.doi.org/10.1016/j.jaridenv.2007.11.013.

Davis, R.R., Pratt, A.D., 1956. Rotational vs. continuous grazing with dairy cows. Ohio Agric. Exp. Stat. Res. Bull. No. 778, 1–20.

Deshmukh, I.K., 2008. A common relationship between precipitation and grassland peak for East and southern Africa. Afr. J. Ecol. 22, 181–186, http://dx.doi.org/10.1111/j.1365-2028.1984.tb00693.x.

Duru, M., Colombani, H., 1992. Haymaking: risks and uncertainty in central Pyrenees grasslands. Agric. Syst. 38, 185–207, http://dx.doi.org/10.1016/0308-521X(92).

Feng, X.M., Zhao, Y.S., 2011. Grazing intensity monitoring in Northern China steppe: Integrating CENTURY model and MODIS data. Ecol. Indic. 11, 175–182, http://dx.doi.org/10.1016/j.ecolind.2009.07.002.

He, C., Zhang, Q., Li, Y., Li, X., Shi, P., 2005. Zoning grassland protection area using remote sensing and cellular automata modeling – a case study in Xilingol steppe grassland in northern China. J. Arid Environ. 63, 814–826, http://dx.doi.org/10.1016/j.jaridenv.2005.03.028.

Heislar-White, J.L., Knapp, A.K., Kelly, E.F., 2008. Increasing precipitation event size increases aboveground net primary productivity in a semi-arid-grassland. Oecologia 158, 129–140, http://dx.doi.org/10.1007/s00442-008-1116-9.

Hodgson, J., Brookes, I.M., 1999. Nutrition of grazing animals. In: White, J., Hodgson, J. (Eds.), New Zealand Pasture and Crop Science. Oxford University Press, London, UK, pp. 117–132.

Hooper, D.U., Johnson, L., 1999. Nitrogen limitation in dryland ecosystems: responses to geographical and temporal variation in precipitation. Biogeochemistry 46, 274–293, http://dx.doi.org/10.1007/BF01007582.

Huang, D., 2001. Impact of grazing on the ecosystems. In: Shiyomi, M., Koizumi, H. (Eds.), Structure and Function in Agroecosystem Design and Management. CRC Press, Boca Raton, USA, pp. 253–273.

Huang, D., Shiyomi, M., Chen, J., Takahashi, S., Hori, Y., Yamamura, Y., Wang, Y., 2004. Spatial heterogeneity of vegetation in Inner Mongolia, China. Grassl. Sci. 50, 319–328.

Kawamura, K., Akiyama, T., Yokota, H., Tsutsumi, M., Yasuda, T., Watanabe, O., Wang, S., 2005. Quantifying grazing intensities using geographic information systems and satellite remote sensing in the Xilingol steppe region, Inner Mongolia, China. Agric. Ecosyst. Environ. 107, 83–93, http://dx.doi.org/10.1016/j.agee.2004.09.008.

Kendall, M.G., 1980. Multivariate Analysis, 2nd ed. Charles Griffin & Co. Ltd., High Wycombe, UK.

Lantinga, E.A., (Ph.D. thesis) 1985. Productivity of Grasslands under Continuous and Rotational Grazing. Wageningen, Lantinga, Holland, pp. 111.

Li, W.N., Ali, S.H., Zhang, Q., 2007. Property rights and grassland degradation: a study of the Xilingol pasture, Inner Mongolia, China. J. Environ. Manage. 85, 461–470, http://dx.doi.org/10.1016/j.jenvman.2006.10.010.

Liu, S., Wang, T., 2007. Aeolian desertification from mid-1970s to 2005 in Otingdag sandy land, north China. Environ. Geol. 51, 1057–1064, http://dx.doi.org/10.1007/s00254-006-0375-1.

Martin, G., Martin-Clouaire, R., Rellier, J.-P., Duru, M., 2011. A simulation framework for the design of grassland-based beef-cattle farm. Environ. Model. Software 26, 371–385, http://dx.doi.org/10.1016/j.envsoft.2010.10.002.

Parton, W.J., 1978. Abiotic section of ELM. In: Innis, E.S. (Ed.), Grassland Simulation Model. Springer-Verlag, New York, USA, pp. 31–53.

Piao, S.L., Fang, J.Y., Zhou, L.M., Tan, K., Tao, S., 2007. Changes in biomass carbon stocks in China's 457 grasslands between 1982 and 1999. Global. Biogeochem. Cycles 21, GB2002, http://dx.doi.org/10.1029/2005GB002634.

Scurlock, J.M.O., Johnson, K., Olson, R.J., 2002. Estimating net primary productivity from grassland biomass dynamics measurements. Global Change Biol. 8, 736–753, http://dx.doi.org/10.1046/j.1365-2486.2002.00512.x.

Shiyomi, M., 1988. Grassland management models. J. Agric. Res. Quart. 22, 214–228.

Shiyomi, M., Kirita, H., Takahashi, S., 2000. Roles of plant biomass and vegetational heterogeneity, and energy-matter cycling in grassland sustainability. Ecol. Model. 132, 135–149, http://dx.doi.org/10.1016/S0304-3800(00)00311-2.

Shiyomi, M., Akiyama, T., Wang, S.P., Yiruhan, Ailikun, Hori, Y., Chen, Z.Z., Yasuda, T., Kawamura, K., Yamamura, Y., 2011. A grassland ecosystem model of the Xilingol steppe, Inner Mongolia. China. Ecol. Model. 222, 2073–2083, http://dx.doi.org/10.1016/j.ecolmodel.2011.03.028.

Swemmer, A.M., Knapp, A.K., Snyman, H.A., 2007. Intra-seasonal precipitation patterns and above-ground productivity in three perennial grasslands. J. Ecol. 95, 780–788, http://dx.doi.org/10.1111/j.1365-2745.2007.01237.x.

ten Berge, H.F.M., Aggarwal, P.K., Kropff, M.J. (Eds.), 1997. Applications of Rice Modelling. Elsevier, Amsterdam, Holland, p. 164.

Thornley, J.H.M., 1998. Grassland Dynamics: An Ecosystem Simulation Model. CAB International, Wallingford, UK, pp. 241.

Tong, C., Wu, J., Yong, S., Yang, J., Yong, W., 2004. A landscape-scale assessment of steppe degradation in the Xilin River Basin, Inner Mongolia, China. J. Arid Environ. 59, 133–149, http://dx.doi.org/10.1016/j.jaridenv.2004.01.004.

Torssell, B.W.R., Kornher, A., 1983. Validation of a yield prediction model for temporary grasslands [Sweden]. Swed. J. Agric. Res. 13, 125–135.

van der Werf, W., Keesman, K., Burgess, P., Graves, A., Pilbeam, D., Incoll, L.D., Metselaar, K., Mayus, M., Stappers, R., van Keulen, H., João Palma, J., Dupraz, C., 2007. Yield-SAFE: a parameter-sparse, process-based dynamic model for predicting resource capture, growth, and production in agroforestry systems. Ecol. Eng. 29, 419–433, http://dx.doi.org/10.1016/j.ecoleng.2006.09.017.

van Dyne, G.M., 1969. Grassland Management, Research, and Training Viewed in a Systems Context. Science Series #3. Colorado State University, Range Science Department, Fort Colins, USA, pp. 50.

Walton, P.D., Martinez, R., Bailey, A.W., 1981. A comparison of continuous and rotational grazing. J. Rangeland Manage. 34, 19–21.

Wang, S.P., 2000. Relationships between body gains and stocking rates and grazing sheep on typical Inner Mongolia grassland. Acta Pratacult. Sinica 9, 10–16 (in Chinese with English abstract).

Wang, S.P., Wang, Y.F., Li, Y.H., Chen, Z.Z., 1998. The influence of different stocking rates on herbage regrowth and aboveground net primary production. Acta Agrestia Sinica 6, 275–281 (in Chinese with English abstract).

Wuyunna, Luo, W., Pei, H., Shiyomi, M., Lu, J., Huo, G., 2012. Climate change and effect on the biomass growth in steppe communities in Kherlon River Basin, Northern China. Acta Ecol. Sinica 32, 215–220, http://dx.doi.org/10.1016/j.chnaes.2012.05.004.

Xie, Y., Sha, Z., Mei, Y.M., Bai, Y., Zhang, L., 2009. A comparison of two models with Landsat data for estimating above ground grassland biomass in Inner Mongolia, China. Ecol. Model. 220, 1810–1818, http://dx.doi.org/10.1016/j.ecolmodel.2009.04.025.

Yiruhan, Hayashi, I., Nakamura, T., Shiyomi, M., 2001. Changes in floristic composition of grassland according to grazing intensity in Inner Mongolia, China. Grassl. Sci. 47, 362–369.

Yiruhan, Ailikun, Ma, Z.G., Shiyomi, M., 2011. Forty-eight-year climatology of air temperature and precipitation changes in Xilingol steppe (Inner Mongolia), China. Grassl. Sci. 57, 168–172, http://dx.doi.org/10.1111/j.1744-697X.2011.00224.x.

Zheng, Y., Xie, Z., Jiang, L., Wu, Y., Shimizu, H., 2006. Model simulation and comparison of the ecological characteristics of three degraded grassland types in China. Belg. J. Bot. 138, 109–118.